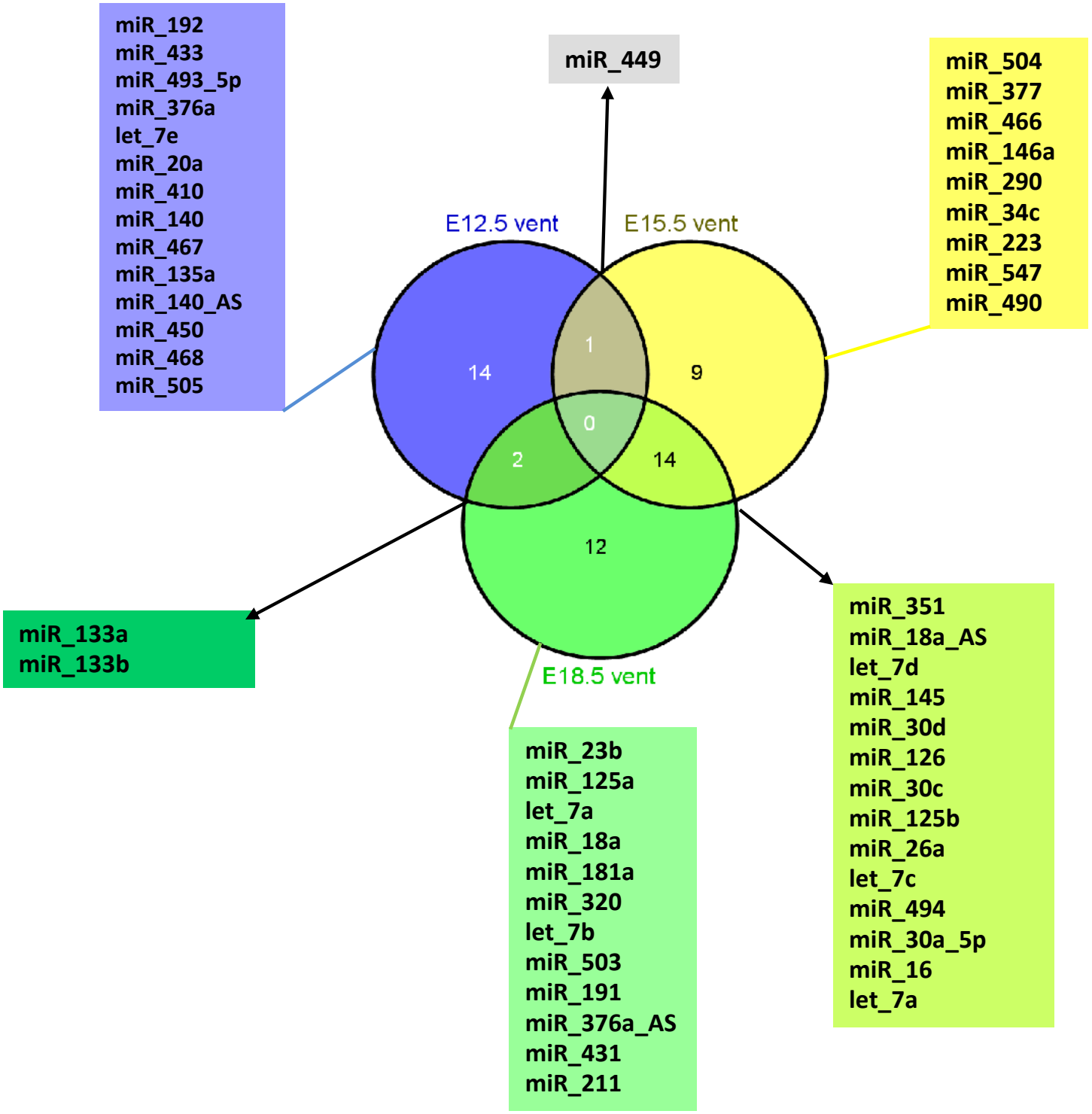

Supplementary Figure 1

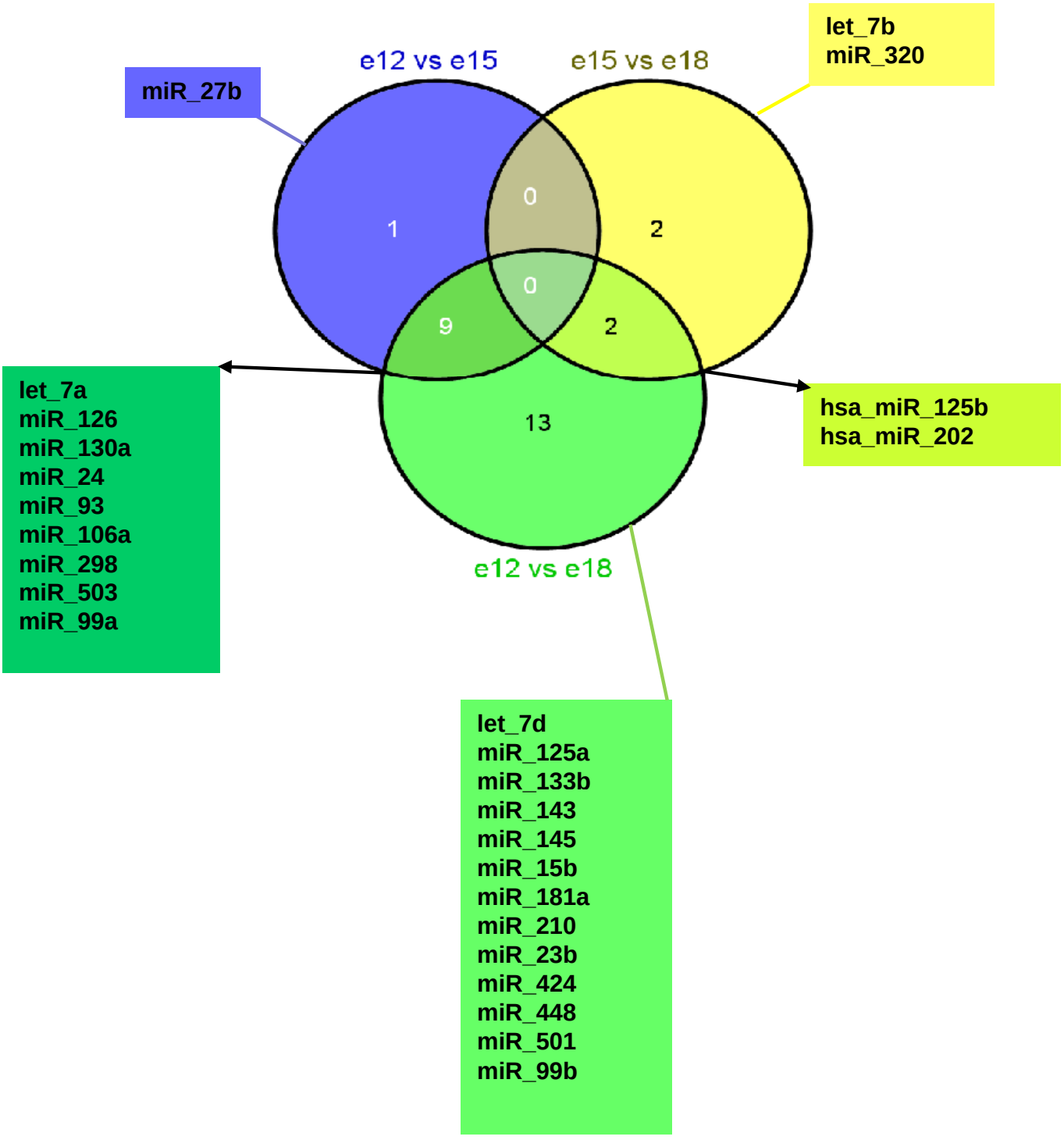

Supplementary Figure 2

E12.5

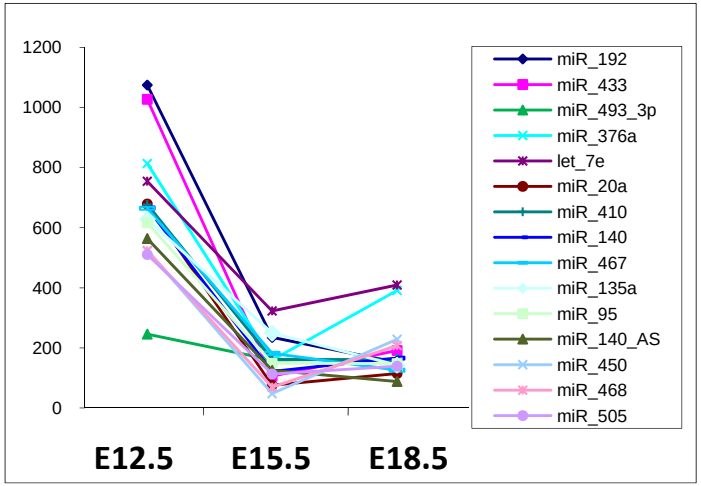

E12.5 and E15.5

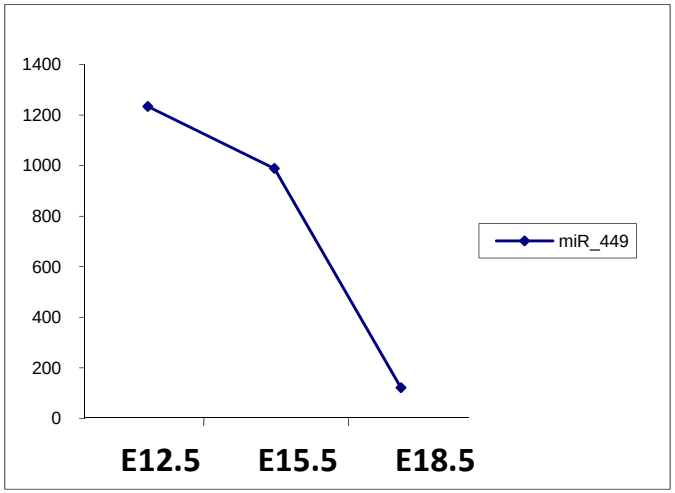

E15.5

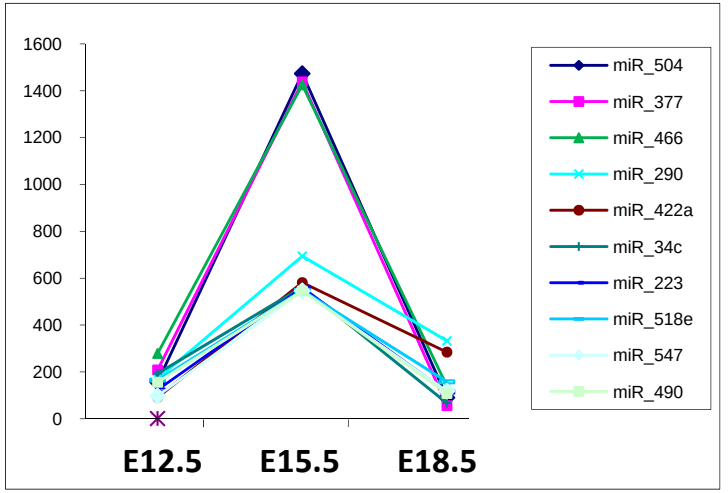

E15.5 and E18.5

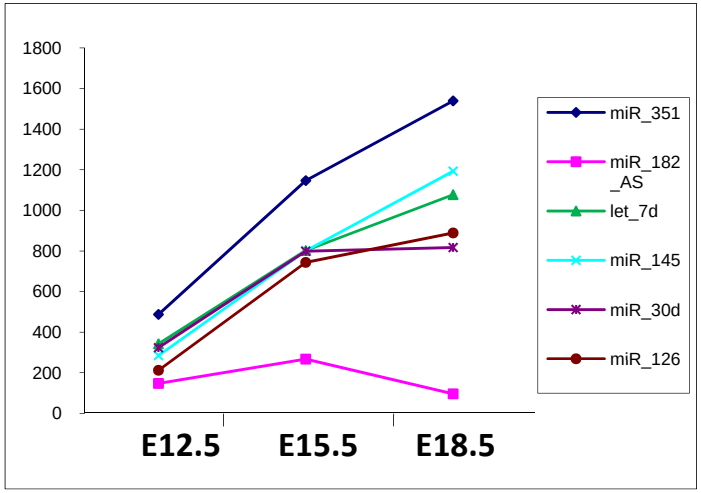

E18.5

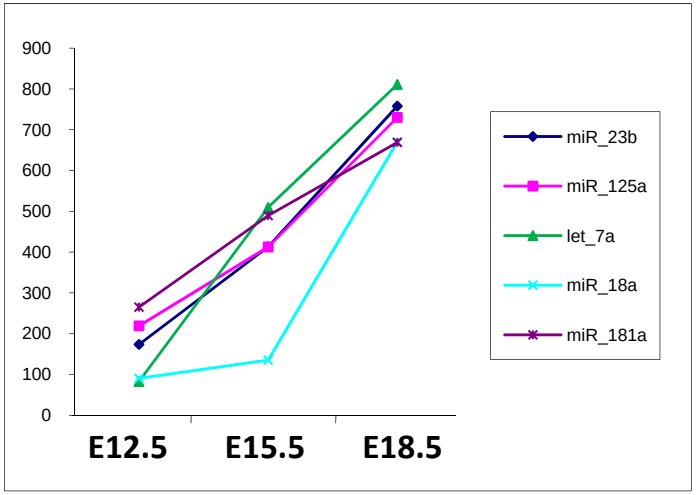

E12.5 and E18.5

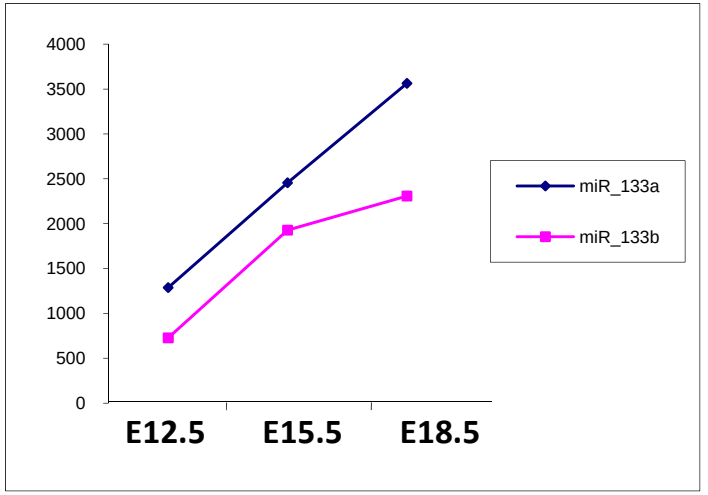

Supplementary Figure 3

E12.5/15.5

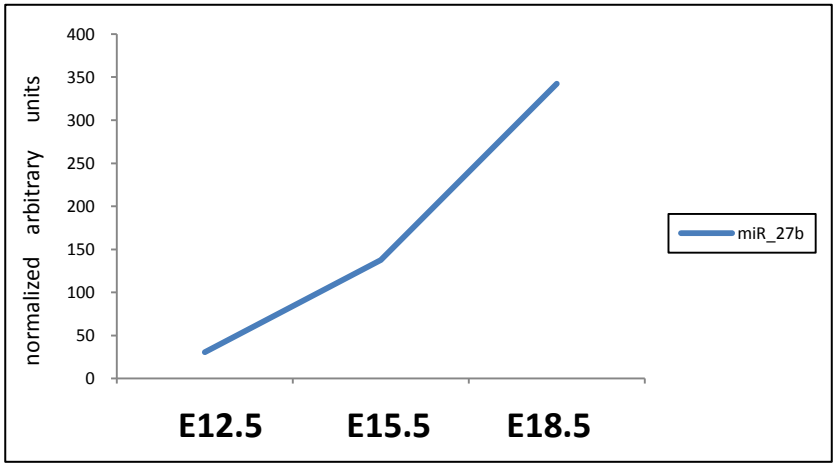

E15.5/E18.5

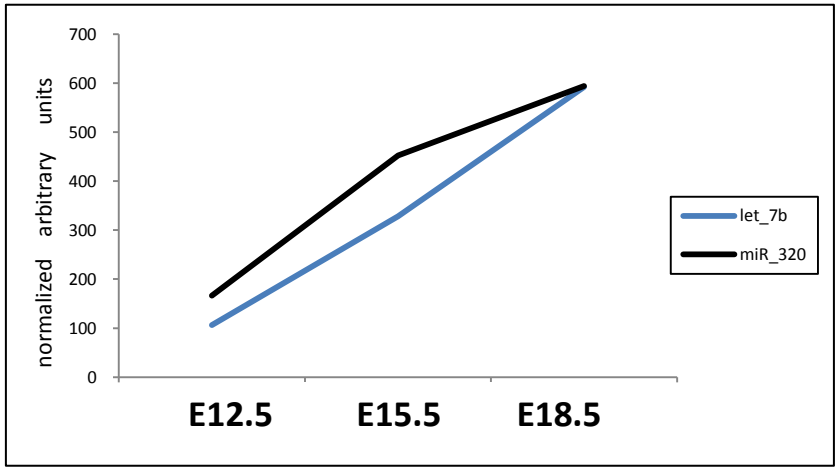

E15.5/E18.5 and E12.5/E18.5

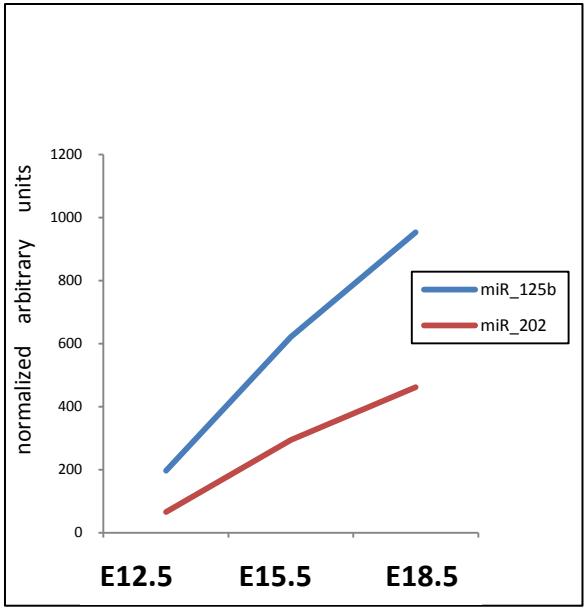

E12.5/E18.5

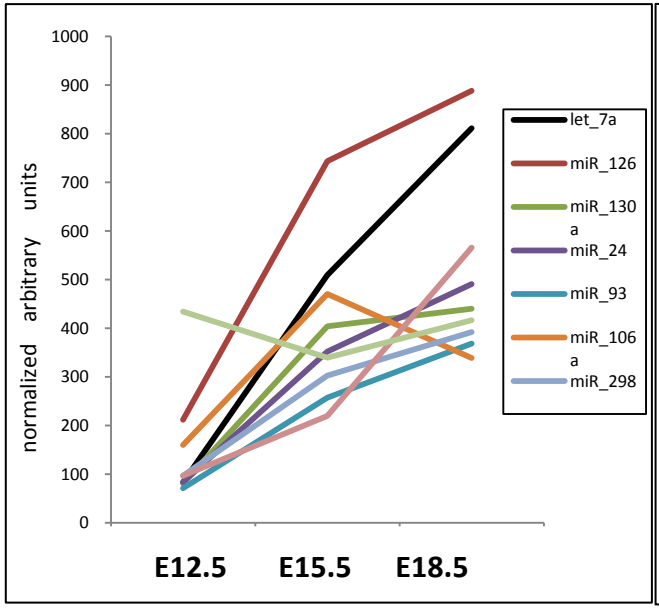

E12.5/E15.5 and E12.5/E18.5

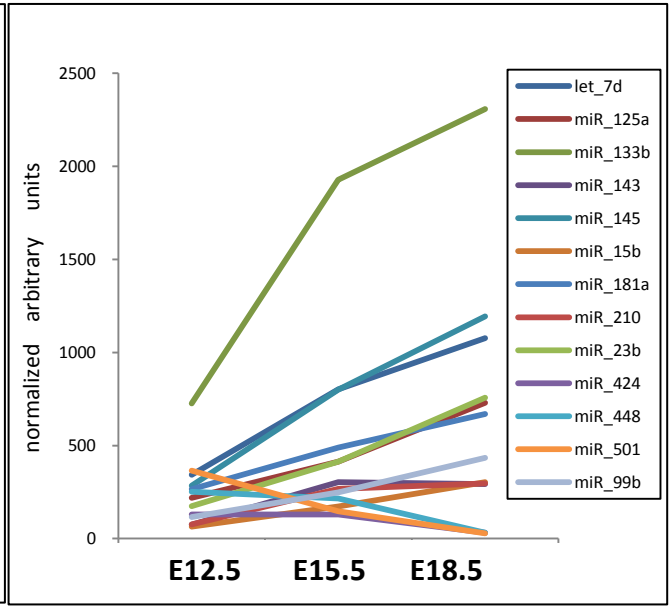

Supplementary Figure 4

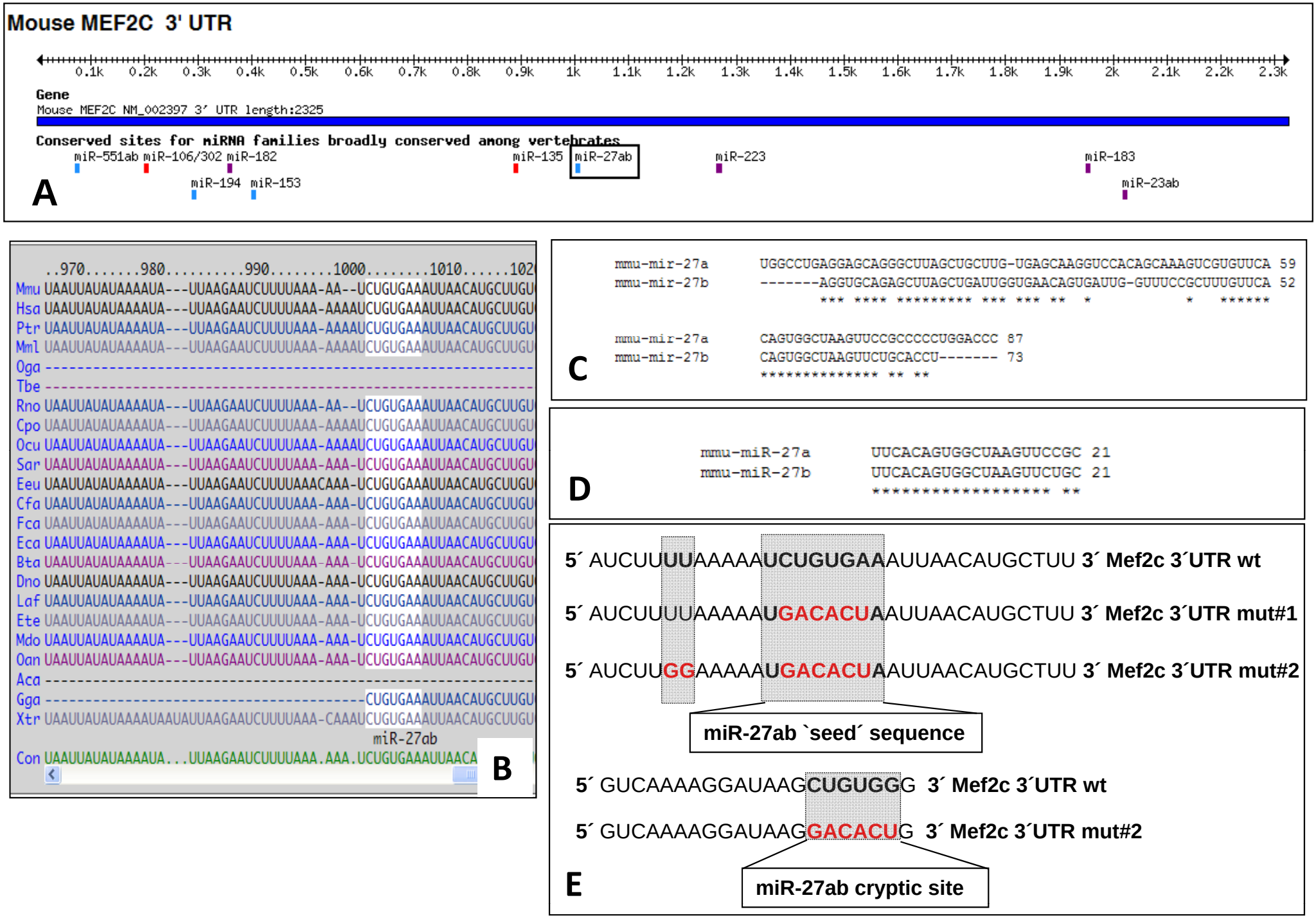

Supplementary Figure 5

Supplementary Materials & Methods

Embryos

C57/BL6 mouse embryos were isolated at three distinct developmental stages (embryonic day (E) 12.5, E15.5 and E18.5). Ventricular chambers corresponding to all the embryos of a single litter were carefully dissected, pooled, snapped frozen in liquid nitrogen and stored at -80ºC until used. Three litters were used for E12.5, corresponding to 14 embryos and two litters were used for E15.5 and E18.5, corresponding to 12 and 8 embryos, respectively. For *in situ* hybridization, pregnant C57/BL6 mouse females were sacrificed at E10.5 and E12.5 and the embryos were gently dissected, briefly fixed in ice-cold 4% freshly-made formaldehyde and dehydrated in graded ethanol steps. Embryos were kept in absolute ethanol at -80ºC until used.

RNA isolation

Total RNA isolation was performed using Trizol reagent (Invitrogen) according to manufacturer's guidelines. Total RNA was used for microRNA microarray analyses. DNAse treatment was performed during 1 hour at 37ºC prior to cDNA synthesis either using SuperScript RT III (Invitrogen) or Exiqon microRNA qRT-PCR detection system.

Microarrays analysis

mirVana microarrays (Ambion) were used to profile microRNA signatures at different developmental stages of ventricular chamber formation. 20 μg of total RNA was used to hybridize each microRNA microarray and two distinct microarrays were assessed per developmental stage analyzed. Each microarray contains quadruplicates of mouse/ human/ rat mature microRNAs identifed to date (~500 microRNAs). microRNA -Cy3 labeling, microarray hybridization and washing steps were performed according to the manufacturer´s guidelines.

In situ hybridization

Embryos were hydrated by incubation in graded ethanol/PBS steps until reaching a pure sterile PBS solution. Embryos were subsequently prehybridized and hybridized overnight with LNA-labeled microRNA probes (Exiqon) for miR-27 and miR-1 as internal hybridization control. Negative controls included embryos that were run entirely through the hybridization protocol but with scrambled LNA negative control probes (Exiqon). In all cases, these negative embryos yield neglible coloration (data not shown). Hybridization and coloration conditions are in essence as described by the manufacturer's guidelines with minor modifications as described by Crist et al. (2009) [1]. Prehybridization and hybridization temperatures were 20ºC less than the indicated Tm of the probe, as recommended by the manufacturer. After the coloration reaction was stopped, all samples were analyzed and photographed and stained embryos were subsequently processed for cryostat sectioning.

Tissue sectioning

Stained embryos were incubated in 30% sucrose in PBS, mounted in OCT embedding media and cryosectioned at 40 microns as previously described by Crist et al., (2009) [43]. Sections were collected in glass slides and mounted with cover slips using DPX mounting medium.

Transfection assays

HL-1 mouse immortalized atrial myocardial ([44] Claycomb et al., 1998) cells and Sol8 skeletal myogenic (ATCC, CRL-2174) cells were used to assay microRNA-27 gain-of-function experiments. HL-1 cells ($6*10^5$ cells per dish) were culture under appropriate cell culture condition ([2] Claycomb et al., 1998) and plated 30mm culture dishes. Sol8 cells (10^5 cells per well) were cultured under growing conditions ([3] Daubas et al., 1988) and plated in 6-well plates. Pre-miR-27, pre-miR-125b and miR-219a (Ambion) were transfected with lipofectamine 2000 (Invitrogen) into HL-1 nd Sol8 cells at 5 nmol according to manufacturer's guidelines, respectively. Negative controls included non transfected cells as well as FAM-labeled pre-miR negative control transfected cells, which also allow evaluation of the transfection efficiency. In all cases, transfection efficiencies were greater than 50%, as revealed by observation of FAM-labeled pre-miR transfection. After 4 hours transfection, HL-1 cells were culture in appropriate cell culture media as reported by Claycomb et al. 1998 [2]. Sol8 cells, after transfection (4 hrs), were allowed recover in a 20% FCS rich Sol8 growing media for one hour and thereafter, transferred again into normal growing medium (10% FCS). Cells were collected 24h (pre-miR treatment) after transfection. Cell transfections for each condition were run in triplicates. Negative control and transfected cells were collected and processed for RNA isolation using Trizol-base standard protocols. RNA quality and integrity was evaluated using a Nanodrop spectrophotometer and cDNAs were retro-transcribed accordingly.

Mef2c 3'UTR DNA Constructs. A 504 nucleotide sequence from the 3'UTR of the Myf5 transcript, encompassing the predicted miR-27 binding site, was amplified by PCR using forward 5'- AAAACTCGAGCCATGCTTTGCTAACCAAGA-3' and reverse 5'-AAAAGCGGCCGCATGAAGAGAGATCTGAAAGG-3' primers, cloned into the *Xho*I-*Not*I sites of pBluescript II SK (+) vector (Stratagene) and the sequence was verified. The predicted miR-27b site was mutated (underlined sequence) with mutagenic primers 5'-TCTTTGTAGAAGTTTTGTTTTTGAAATGTGTATTTCTAATTATATAAAATATTAAGAATCTTTTAAAAATGACACTAATTAACATGCTTGTGTATAGCTTTCTAATATATATAA -3', and 5'-GTTTTGTTTTTGAAATGTGTATTTCTAATTATATAAAATATTAAGAATCTAGGTAAAATGACACTAATTAACATGCTTGTGTATAGCTTTCT-3'. An additional, non-canonical site was also mutated with mutagenic primer 5'-TATAAGTTCAAGGTCAGCTGTCAAAAGGATAAGGACACTGGTTAGAACATATTACATTGCAAC

ATCCTAAAT-3'. Mutations were performed with the Quickchange Multi-site mutagenesis kit (Stratagene), and mutations were confirmed by sequence analysis. The wild-type and mutated 3'UTRs were subcloned into the *Xho*I-*Not*I site of the psicheck-2 vector (Promega).

qRT-PCR analysis

Quantitative qRT-PCR for mRNA analyses was performed as previously described ([4] Dominguez et al., 2008). All reactions were always run in triplicates where Mef2c expression levels (forward 5´->3´ AGAAGAAACACGGGGACTATGGG; reverse 5´->3´ GGGGTGAGTGCATAAGAGGAG), Scn5a (forward 5´->3´ GGA GTA CGC CGA CAA GAT GT; reverse 5´->3´ ATC TCG GCA AAG CCT AAG GT) and Scn1b (forward 5´->3´ TGC TCA TTG TGG TGT TGA CC ; reverse 5´->3´ CCT GGA CGC CTG TAC AGT TT) were normalized against three distinct controls, i.e. beta-actin (forward 5´->3´ ; reverse 5´->3´), Gusb (forward 5´->3´ ACTCTCAGCGGTGACTGGTT; reverse 5´->3´ ACGCATCAGAAGCCGATTAT) and Gapdh (forward 5´->3´ TCTTGCTCAGTGTCCTTGCTGG; reverse 5´->3´ TCCTGGTATGACAATGAATACGGC). In all cases, similar trends were observed and thus normalization only against Gapdh is illustrated. Represented values correspond to the mean value obtained from three independent transfection experiments, and the corresponding standard deviation is depicted in the corresponding graphs. miR-27b microRNA qRT-PCR was performed using Exiqon LNA microRNA qRT-PCR primers and detection kit according to manufacturer's guidelines. All reactions were run in triplicates using 5S as normalizing control, as recommended by the manufacturer. SyBR Green was used as quantification system on a Stratagene Q-Max 2005P qRT-PCR thermocycler. Relative measurements were calculated as described by Livak & Schmittgen (2001)[5] and control measurements were normalized to represent 100%.

Statistical and bioinformatics analysis

MicroRNA microarray statistical analysis was performed by calling corresponding Bioconductor functions (http://www.bioconductor.org/) in R software (http://www.r-project.org/). Densitometry values < 1 were first imputed using the KNN algorithm implemented in the Bioconductor *impute* package (http://bioconductor.org/packages/2.0/bioc/html/impute.html) and all data were further transformed to the logarithmic scale (log2). To minimize technical (non-biological) variability among arrays, data were then normalized using the quartiles normalization function implemented in the Bioconductor *limma* package (http://bioconductor.org/packages/2.0/bioc/html/limma.html). Statistically significant differences between groups were identified using the t-test and multiple hypothesis correction (FDR) implemented in the multitest package (http://www.bioconductor.org/packages/2.2/bioc/html/multtest.html). Hierarchical clustering, an unsupervised way of grouping samples based only on their gene expression similarities, was carried out using Cluster and TreeView software (http://rana.lbl.gov/EisenSoftware.htm). Venn diagrams were drawn with VENNY (http://bioinfogp.cnb.csic.es/tools/venny/index.html).

qRT-PCR data statistical analyses were performed using unpaired Student t- test. Significance level or p values are stated on each corresponding figure legend.

References

[1]. Crist CG, Montarras D, Pallafacchina G, Rocancourt D, Cumano A, Conway SJ, Buckingham M. Muscle stem cell behavior is modified by microRNA-27 regulation of Pax3 expression. *Proc Natl Acad Sci U S A*. 2009;**106**:13383-13387.

[2]. Claycomb WC, Lanson NA Jr, Stallworth BS, Egeland DB, Delcarpio JB, Bahinski A, Izzo NJ Jr. HL-1 cells: a cardiac muscle cell line that contracts and retains phenotypic characteristics of the adult cardiomyocyte *Proc Natl Acad Sci U S A*. 1998;**95**:2979-2984.

[3]. Daubas P, Klarsfeld A, Garner I, Pinset C,Cox R, Buckingham M. Functional activity of the two promoters of myosin alkali light chain gene in primary muscle cell cultures: comparison with other muscle gene promoters and other culture system. *Nucleic Acids Res* 1988;**16**:1251–1271.

[4]. Domínguez JN, de la Rosa A, Navarro F, Franco D, Aránega AE. Tissue distribution and subcellular localization of the cardiac sodium channel during mouse heart development. *Cardiovasc Res*. 2008;**78**:45-52.

[5]. Livak KJ, Schmittgen TD. Analysis of relative gene expression data using real-time quantitative PCR and the 2(-Delta Delta C(T)) Method. *Methods*. 2001;**25**:402-408.

Supplementary data Figure legends

Supplementary Figure 1. Venn diagram representation of the most abundantly expressed microRNAs at E12.5, E15.5 and E18.5 in mouse ventricular chambers. Among those microRNA abundantly expressed during ventricular development, 14 microRNAs are highly expressed at E12.5, while only one remains to be highly expressed also at E15.5. 9 microRNAs are highly expressed at E15.5, while 12 more remain to be also highly expressed at 18.5. Interestingly, we have found no microRNA that is always highly expressed at these three distinct developmental stages. Only two microRNAs display steadily increasing levels (miR-133a/miR133b).

Supplementary Figure 2. Venn diagram representation of differentially expressed microRNAs at E12.5, E15.5 and E18.5 mouse ventricular chambers. Among those microRNAs differentially expressed, miR-27's differential expression is at early developmental stages (E12.5).

Supplementary Figure 3. Graphical representation of the expression profiles during cardiogenesis of the most abundantly expressed microRNAs at E12.5, E15.5 and E18.5 mouse ventricular chambers as listed in Supplementary Figure 1.

Supplementary Figure 4. Graphical representation of the expression profiles during cardiogenesis differentially expressed microRNAs at E12.5, E15.5 and E18.5 mouse ventricular chambers as listed in Supplementary Figure 2.

Supplementary Figure 5. TargetScan analyses of putative microRNA binding sites in the mouse Mef2c transcription factor 3´UTR. As can be observed, miR-27ab is a putative microRNA targeting Mef2c (panel A), and its binding site is highly conserved along the Mef2c 3´UTRs in other species (panel B). Panel C displays a sequence comparison between pre-miR-27a and pre-miR-27b. Panel D displays a sequence comparison between miR-27a and miR-27b. Note that although the pre-miR sequences are partially divergent, the mature miRs are almost similar, with a single nucleotide mismatch and identical seed sequence (blue shadowed). Thus, the predicted targets are the same for miR-27a and miR-27b. Panels E illustrates the region of the 3´UTR of the Mef2c gene which harbors the endogenous miR-27 binding sequence (wild-type; Mef2c 3´UTR wt) and the mutated sequences (Mef2c 3´UTR mut#1 and Mef2c 3´UTR mut#2) of the miR-27 seed sequence that have been used in the luciferase reporter analyses. The upper bold boxed sequence corresponds to the miR-27 seed sequence and the red highlighted sequences are the mutated sequences. In addition, Mef2c 3´UTR mut#2 construct also harbors a mutated miR-27 cryptic site, as depicted in the lower bold boxed sequence.

Supplementary Table I. List of statistically significant microRNAs differentially expressed ($p<0.05$) between E12.5, E15.5 and E18.5 mouse ventricular cardiac chambers. FC represents the fold change.

Supplementary Table II. Chromosomal location and genetic locus of those microRNAs that display statistically significant differences (as provided in Table I) between E12.5, E15.5 and E18.5 mouse ventricular cardiac chambers.

SupplementaryTable III. Chromosomal location and genetic locus of those microRNAs that display the most abundant expression at E12.5, E15.5 and E18.5 in mouse ventricular cardiac chambers.

E12.5 versus E15.5	
p<0.05	**FC**
let_7a	**6,145539636**
miR_126	**3,506700253**
miR_130a	**6,145539636**
miR_24	**4,20407817**
miR_27b	**4,49014276**
miR_93	**3,621136428**
miR_106a	**4,714827958**
miR_298	**3,13028595**
miR_503	**6,522242554**
miR_99a	**5,005612932**

E15.5 versus E18.5	
p<0.05	**FC**
let_7b	**1,80245018**
miR_125b	**1,5347432**
miR_202	**1,57303475**

E12.5 versus E18.5	
p<0.05	**FC**
let_7a	**9,783145399**
let_7d	
miR_125a	**3,331788945**
miR_125b	**4,8391763**
miR_126	**4,190646834**
miR_130a	**5,421393618**
miR_133b	**3,176657825**
miR_143	**3,89385226**
miR_145	**4,190171302**
miR_15b	**4,726468475**
miR_181a	**2,71098605**
miR_198	**15,38929848**
miR_202	**7,067497594**
miR_210	**3,879625074**
miR_23b	**4,359569189**
miR_24	**5,861478384**
miR_26a	**2,705261188**
miR_424	**-4,00985929**
miR_448	**-7,85281573**
miR_501	**-13,0999792**
miR_513	**6,279207279**
miR_93	**5,186746453**
miR_99b	**3,748631663**
miR_106a	**4,845756666**
miR_298	**4,052966794**
miR_503	**3,783747611**
miR_99a	**6,51752868**

Chinchilla et al., Supplementary Table I

microRNA	Chromosomal location	Gene locus
let_7a	13: 48633548-48633641 [-]	intergenic
let_7a	13: 48633548-48633641 [-]	intergenic
let_7b	15: 85537749-85537833 [+]	intergenic
let_7c	16: 77599902-77599995 [+]	ENSMUST00000114231 ; intron 1
let_7d	13: 48631381-48631483 [-]	intergenic
let_7e	17: 17967316-17967408	intergenic
miR_125a	17: 17967776-17967843 [+]	intergenic
miR_125b	9: 41390009-41390085 [+]	2610203C20Rik; intron 2
miR_126	2: 26446877-26446949 [+]	Egfl7-007; intron 1
miR_133a	18: 10782907-10782974 [-]	Mib1; intron 12
miR_133b	1: 20672850-20672968 [+]	intergenic
miR_135a	9: 106056455-106056544	Glycerate kinase 3'UTR
miR_140	8: 110075144-110075213	Wwp2 (WW dc E3 ubiquitin protein ligase 2)
miR_140_AS	8: 110075144-110075213	Wwp2 (WW dc E3 ubiquitin protein ligase 2)
miR_145	18: 61807479-61807548 [-]	intergenic
miR_146a	11: 43187899-43187963	intergenic
miR_16	14: 62250717-62250809 [-]	intergenic
miR_181a	2: 38708255-38708330 [+]	Nr6a1-002; intron 2
miR_18a	14: 115443073-115443168 [+]	intergenic
miR_18a_AS	14: 115443073-115443168 [+]	intergenic
miR_191	9: 108470650-108470723 [+]	intergenic
miR_192	19: 6264844-6264932	intergenic
miR_20a	14: 115443379-115443485	intergenic
miR_211	7: 71350692-71350797 [+]	Trpm1-004; intron 4
miR_223	X: 93438156-93438265	intergenic
miR_23b	13: 63401792-63401865 [+]	ENSMUST00000060660 ; intron 1
miR_26a	9: 118940914-118941003 [+]	Ctdspl; intron 5
miR_290	7: 3218627-3218709	intergenic
miR_30a_5p	1: 23279108-23279178 [+]	intergenic
miR_30c	4: 120442139-120442227 [-]	Nfyc-006; intron 3
miR_30d	15: 68172770-68172851 [-]	intergenic
miR_320	14: 70843317-70843398 [+]	intergenic
miR_34c	4: 149442563-149442664	intergenic
miR_351	X: 50406432-50406530 [-]	intergenic
miR_376a	12: 110961991-110962058	intergenic
miR_376a_AS	12: 110961991-110962058 [+]	intergenic
miR_377	12: 110978720-110978787	intergenic
miR_410	12: 110981925-110982005	intergenic
miR_431	12: 110828657-110828747 [+]	Rtl1; exon 1
miR_433	12: 110829925-110830048	Rtl1 (retrotransposon-like 1)
miR_449	13: 113827742-113827832	similar to CDC20-like protein, intron 2
miR_450	X: 50401331-50401421	intergenic
miR_466	2: 10429545-10429617	Sfmbt2-01; intron 10
miR_467	2: 10397973-10398045	Sfmbt2-01 (Scm-like with four mbt domains 2)
miR_468	6: 81846593-81846670	intergenic
miR_490	6: 36371742-36371825	intergenic
miR_493_5p	12: 110818443-110818525	intergenic
miR_494	12: 110953528-110953612 [+]	intergenic
miR_503	X: 50407161-50407231 [-]	intergenic
miR_504	X: 56350835-56350913	Fgf13; intron 3
miR_505	6: 81846593-81846670	Atpase, class VI, type 11C
miR_547	X: 65241549-65241626	intergenic

Chinchilla et al., Supplementary Table II

microRNA	Chromosomal location	Gene locus
let_7a	13: 48633548-48633641 [-]	intergenic
let_7a	13: 48633548-48633641 [-]	intergenic
let_7b	15: 85537749-85537833 [+]	intergenic
let_7d	13: 48631381-48631483 [-]	intergenic
miR_106a	X: 50095680-50095744 [-]	Kis2-002; exon 2
miR_106a	X: 50095680-50095744 [-]	Kis2-002; exon 2
miR_125a	17: 17967776-17967843 [+]	RP23-77H6.2-003; exon 1
miR_125b	9: 41390009-41390085 [+]	2610203C20Rik-201; intron 2
miR_125b	9: 41390009-41390085 [+]	2610203C20Rik-201; intron 2
miR_126	2: 26446877-26446949 [+]	Egfl7-007; intron 7
miR_126	2: 26446877-26446949 [+]	Egfl7-007; intron 7
miR_130a	2: 84581272-84581335 [-]	intergenic
miR_130a	2: 84581272-84581335 [-]	intergenic
miR_133b	1: 20672850-20672968 [+]	intergenic
miR_143	18: 61808850-61808912 [-]	intergenic
miR_145	18: 61807479-61807548 [-]	intergenic
miR_15b	14: 62250864-62250947 [-]	intergenic
miR_181a	1: 139863032-139863118 [+]	intergenic
miR_202	7: 147143588-147143659 [-]	AC107822.6-001; exon 2
miR_202	7: 147143588-147143659 [-]	AC107822.6-001; exon 2
miR_210	7: 148407283-148407392 [-]	intergenic
miR_23b	13: 63401792-63401865 [+]	intergenic
miR_24	13: 63402516-63402583 [+]	AC130827.2-002; intron 3
miR_24	13: 63402516-63402583 [+]	AC130827.2-002; intron 3
miR_26a	9: 118940914-118941003 [+]	Ctdspl-201; intron 5
miR_27b	13: 63402020-63402092 [+]	AC130827.2-002; intron 3
miR_298	2: 174093005-174093086 [-]	intergenic
miR_298	2: 174093005-174093086 [-]	intergenic
miR_448	X: 143592753-143592864 [+]	Htr2c-002; intron 4
miR_501	X: 6818369-6818477 [-]	Clcn5-003; intron 2
miR_503	X: 50407161-50407231 [-]	intergenic
miR_503	X: 50407161-50407231 [-]	intergenic
miR_93	5: 138606751-138606838 [-]	Mcm7-010; exon 1
miR_93	5: 138606751-138606838 [-]	Mcm7-010; exon 1
miR_99a	16: 77599181-77599245 [+]	AC122451.3-201; intron 1
miR_99a	16: 77599181-77599245 [+]	AC122451.3-201; intron 1
miR_99b	17: 17967152-17967221 [+]	intergenic

Chinchilla et al., Supplementary Table III